Materials and Design 86 (2015) 198–203

Contents lists available at ScienceDirect

Materials and Design

journal homepage: www.elsevier.com/locate/jmad

Preparation of titania covered multi-walled carbon nanotube thin films

Zoltán Németh [a,b], Endre Horváth [c], Arnaud Magrez [c], Balázs Réti [a], Péter Berki [a], László Forró [c], Klára Hernádi [a,*]

[a] Department of Applied and Environmental Chemistry, University of Szeged, Rerrich Béla tér 1, Szeged H-6720, Hungary
[b] Laboratory of High Performance Ceramics, Swiss Federal Laboratories for Materials Science and Technology, Überlandstrasse 129, Dübendorf CH-8600, Switzerland
[c] Laboratory of Physics of Complex Matter, École Polytechnique Fédérale de Lausanne, Ecublens CH-1026, Switzerland

ARTICLE INFO

Article history:
Received 11 February 2015
Received in revised form 8 June 2015
Accepted 10 July 2015
Available online 14 July 2015

Keywords:
MWCNT
Sealed system
Relative humidity
SEM
Raman spectroscopy

ABSTRACT

The aim of this work was to investigate the effects of relative humidity on the formation of titania layers on the surface of multi-walled carbon nanotubes under regulated conditions in a sealed system. Reactive precursor compounds such as titanium (IV) oxychloride hydrochloric acid and titanium (IV) bromide were used as precursor to cover the surface of multi-walled carbon nanotubes (MWCNTs) under solvent conditions. The mixtures of MWCNTs and titania compounds were not stirred or sonicated. The effect of relative humidity was influenced using the mixture of sulphuric acid and water in desiccators. As-prepared titan-dioxide (TiO_2) layers were characterized by scanning electron microscopy (SEM), energy dispersive X-ray spectroscopy (EDS), thermogravimetric analysis (TG), X-ray diffraction (XRD) and Raman spectroscopy. Our results revealed that TiO_2 layers with different thicknesses can be obtained using this simple sealed system. These TiO_2 covered multi-walled carbon nanotube films can be ideal candidates for different kinds of applications (e.g. sensors, virus filtration or catalysts).

1. Introduction

Carbon nanotubes (CNTs) have exceptional properties of strength, high surface area, thermal stability, optical activity, thermal and electrical conductivity [1], thereby resulting in many potential applications [2,3]. Due to their high specific surface area and adsorption capability CNTs have been increasingly used in environmental applications [4]. Recently, multi-walled and single-walled CNT filters were developed and found to be effective for multilog microbial removal from contaminated water by physical straining, puncture and depth filtration [5–8]. Furthermore, Gao et al. [9] reported a mechanically stable, electrically conductive and flexible CNT-PVDF membrane and demonstrated that the filter can be effective and efficient for single pass nitrobenzene mineralization by sequential reduction-oxidation.

Combining their remarkable electrical, thermal and mechanical properties with other special properties of conjugated components is also a promising direction to constitute composite materials [10] for nanotechnological and environmental applications such as solar cells, nanoelectric devices, fuel cells, hydrogen storage, adsorptive and degradative water treatment, etc. [11]. In the last couple of years many chemical researches were concerned with the combination of carbon nanotubes with polymers or metal-oxide nanoparticles [12,13]. The applications of these composite materials are very extensive, which usually determines the performance of the composites. The well-known TiO_2 is one of the most important n-type semiconductor materials, which is applied as white pigment, catalyst and/or support owing to its excellent physical and chemical properties [14]. Since CNTs can show good electrical conductivity and with their properties mentioned before, they are excellent candidates to be supports for TiO_2-based nanocomposites to be used as filters for virus removal from water [15] or photocatalysts [16].

TiO_2-MWCNT nanocomposites have been prepared by a number of different techniques including sol–gel synthesis of TiO_2 in the presence of CNTs [17,18], electro-spinning method [19], electrophoretic deposition [20], hydrothermal treatment [21,22], hydrolysis [23], chemical vapor deposition (CVD) [24], dip-coating [25] and layer-by-layer (LBL) technique [26].

The uniformity of the TiO_2 coating and the physical properties of the composite materials may vary depending on the applied preparation method. Though homogeneous coating of TiO_2 on CNTs may be achieved by CVD and electro-spinning methods, these techniques are not simple. They require specialized equipment and it may be difficult to quantify the ratio between composite compounds. Sol–gel method is still the most preferred one, although they usually lead to a heterogeneous, non-uniform coating of CNTs by TiO_2, showing bare CNT surfaces and random aggregation of TiO_2 onto the CNT surfaces [16]. Yu et al. studied the synthesis of TiO_2-MWCNT heterojunction arrays on Ti substrate with a controllable thickness of TiO_2 layer for photodegradation of phenol [27]. Wang et al. used a modified sol–gel method to prepare TiO_2-MWCNT nanocomposites that exhibited photocatalytic activity under both UV and visible light [28]. Eder and Windle reported the preparation of CNT–TiO_2 hybrid material and the key achievement of this work was the control of morphology and structure of the TiO_2 coating on the surface of CNTs [29]. An et al. [30] deposited anatase TiO_2

* Corresponding author.
E-mail address: hernadi@chem.u-szeged.hu (K. Hernádi).

http://dx.doi.org/10.1016/j.matdes.2015.07.048
0264-1275/

onto MWCNTs via hydrolysis of titanium isopropoxide in supercritical ethanol and investigated the photocatalytic activity of the composites. Sol–gel technique was utilized to deposit anatase TiO_2 thin films on the grown MWCNTs. $TiCl_4$ was added dropwise to absolute ethanol with a volume ratio of 1/20 while it was stirred. Since $TiCl_4$ shows a strong reaction with water and even humid air, usually TiO_2 is produced by hydrolysis of chemically pure $TiCl_4$ in absolute ethanol [31]. Recently we have reported the preparation of MWCNT based TiO_2 composites using organometallic [32] and inorganic [33] titanium compounds as precursors by a simple impregnation technique. It was demonstrated that the speed of the hydrolysis of precursors highly affects the quality and homogeneity of the titanium layers on the surface of MWCNTs. In accordance with the purpose the coating may consist of separated titania nanoparticles [30] or can be fully homogeneous [31] depending on the applied precursor compound and the speed of the hydrolysis process. In addition, the aforementioned methods of fabricating CNT/TiO_2 nanocomposites have been mostly used for the generation of bulk nanocomposites and do not provide a straightforward method for creating conformal thin films and coatings with precisely regulated composition and properties. Based on our previous results [30,31] a sealed system is proposed in order to investigate the effect of hydrolysis more accurately by changing the relative humidity and to avoid standalone inorganic particles as a side product. The generation of TiO_2/MWCNT thin films would enhance the utility of these nanocomposites in various applications.

In this study, TiO_2/MWCNT nanocomposite membranes were prepared by a modified hydrolysis method. The aim of our work was to elaborate a controlled and regulated process which provides different thickness and homogeneity of TiO_2 layers on the surface of multi-walled carbon nanotubes thereby improving the physical and chemical properties of composite materials. Using this process completely covered MWCNTs could be produced in large quantities, which were strongly influenced by the applied relative humidity values. The resulting thin films can be used in further applications. One of our main goals in the near future is to develop innovative nanocomposite based depth filters to investigate surface properties and adsorption capability in order to improve drinking water quality by removing viruses from contaminated water.

2. Experimental

2.1. Materials

MWCNTs were prepared with the chemical vapor deposition (CVD) technique: acetylene was decomposed in a rotary oven at 720 °C using Fe,Co/$CaCO_3$ as catalyst [34]. Using this synthesis method only MWCNTs were formed without amorphous carbon or other carbonaceous particles [35]. Fig. 1a and b shows SEM image and the Raman spectrum of pristine MWCNTs. The spectrum shows strong peaks at 1342.7 cm^{-1}, 1572.2 cm^{-1} and 2680.1 cm^{-1} which correspond with the D, G and G′ peaks of MWCNTs [36]. There are also weak second-order peaks at 2443.9 cm^{-1}, 2917.3 cm^{-1} and 3220.0 cm^{-1}. The intensity ratios between the three main peaks ($I_D/I_G = 0.51$, $I_{G'}/I_G = 0.69$ and $I_D/I_{G'} = 0.74$) indicate good sp^2 structure and confirm the high-quality of multi-wall carbon nanotubes. The following precursor compounds were used: $TiBr_4$ (Aldrich) and $TiOCl_2 \times 2HCl$ (Aldrich), and ethanol (EtOH) was applied as solvent (HPLC grade from Reanal). PVDF filter membranes (pore size: 0.1 μm, diameter: 47 mm) (Aldrich) were used to prepare MWCNT films. The relative humidity was regulated by changing the concentration of sulphuric acid (H_2SO_4 — Aldrich) – (distilled) H_2O mixtures in different desiccators.

2.2. Preparation of MWCNT based films

First, 50 mg of purified MWCNTs was added into 500 cm^3 EtOH and then it was suspended via sonication for 10 min. In the next step 100 cm^3 portions of this suspension was filtered through a PVDF membrane in order to prepare a MWCNT film. In the meantime calculated amount of precursor compound (15 mg of $TiBr_4$ or 26 mg of $TiOCl_2 \times 2HCl$) was dissolved in 20 cm^3 EtOH. In the following step the MWCNT film and the previously prepared solution of the precursor were put into a beaker. Desiccators were applied in order to investigate the effect of relative humidity (RH) and the ratio of the sulphuric acid and distilled water were changed inside the desiccators to obtain different RH values [37]. The applied RH values were ranged from 10% to 60%. As the final step we putted the beaker inside the desiccator and closed it for 24 h. The as prepared MWCNT film was dried at 50 °C for 12 h.

2.3. Sample characterization

For qualitative characterization the obtained films were investigated by scanning electron microscopy. SEM investigation was performed by a Hitachi S-4700 Type II FE-SEM operating in the range of 5–15 kV. Prior to the measurement the samples were mounted on a conductive carbon tape and these were coated with a thin Au/Pd layer in Ar atmosphere. The energy-dispersive X-ray spectroscopy (EDS) measurement was completed by the scanning electron microscope and a Röntec XFlash Detector 3001 SDD device. Thicknesses of as-prepared TiO_2 layers were investigated using iTEM software from Olympus Soft Imaging Solutions. Thermogravimetric analysis (TG) measurements were performed by a NETZSCH STA 409 PC device in airflow (temperature range: 25–1000 °C, heating rate: 10 °C/min, flow rate: 40 cm^3/min). Based on the results of TGA the heat treatment was performed in Type F21100 Tube Furnace applying quartz boat, quartz tube, and N_2 atmosphere. Nanocomposite samples were annealed at 700 °C for 3 h. The crystalline structure of the inorganic layer was also studied by powder X-ray diffraction method – XRD – by a Rigaku Miniflex II Diffractometer

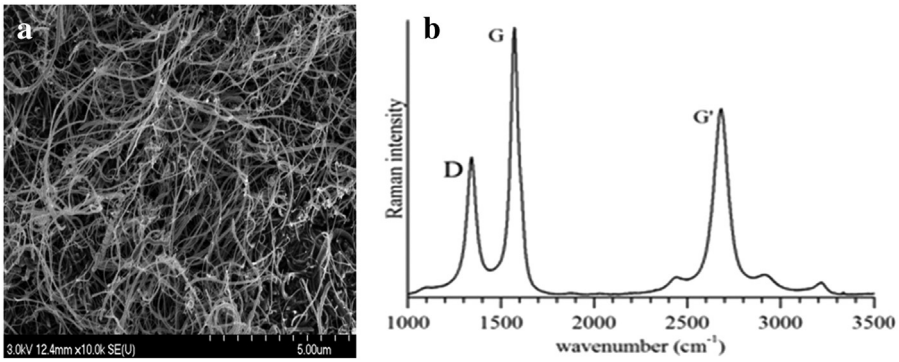

Fig. 1. SEM micrograph (a) and Raman spectrum (b) of pristine MWCNTs.

(angle-range: θ = 10–70°) utilizing characteristic X-ray (CuKα) radiation. Raman spectroscopy measurements were carried out by Thermo Scientific DXR Raman microscope with a 532 nm laser (5 mW).

3. Results and discussion

3.1. Heat treatment and crystal structure analysis

In order to identify the TiO_2 coating and also to transform the amorphous phase into crystalline phase, the composite samples were heat treated. Before that the TG gave us important information about the phase transformations which occurred because of the rise of the temperature (Fig. 2a). Desorption of the residual solvent and water can be observed at temperatures up to 250 °C. A significant weight loss can be noticed beginning at 500 °C which belongs to the burning of MWCNTs. The TGA curve shows two important transformations of TiO_2 as well. The first one starts below 400 °C when TiO_2 particles in anatase phase start to form, and the second transformation occurs at around 700 °C when the anatase phase is transformed into rutile particles. As it is reported in our earlier papers anatase composites were already prepared successfully [30,31]. As in this case rutile phase TiO_2 was preferred, the heat treatment – based on the TG results – was performed at 700 °C for 1 h in N_2 atmosphere using a tubular furnace. Inert atmosphere was necessary to prevent the CNTs burning (burn threshold is around 500 °C in the presence of oxygen – Fig. 2a).

The crystallization of the TiO_2/MWCNT composite samples prepared in different relative humidity worked properly; only one representative XRD pattern is shown (Fig. 2b) here. It is difficult to detect the characteristic reflections of MWCNTs in the XRD patterns because the reflection (110) of TiO_2 and the main reflection of MWCNTs are partly overlapped,

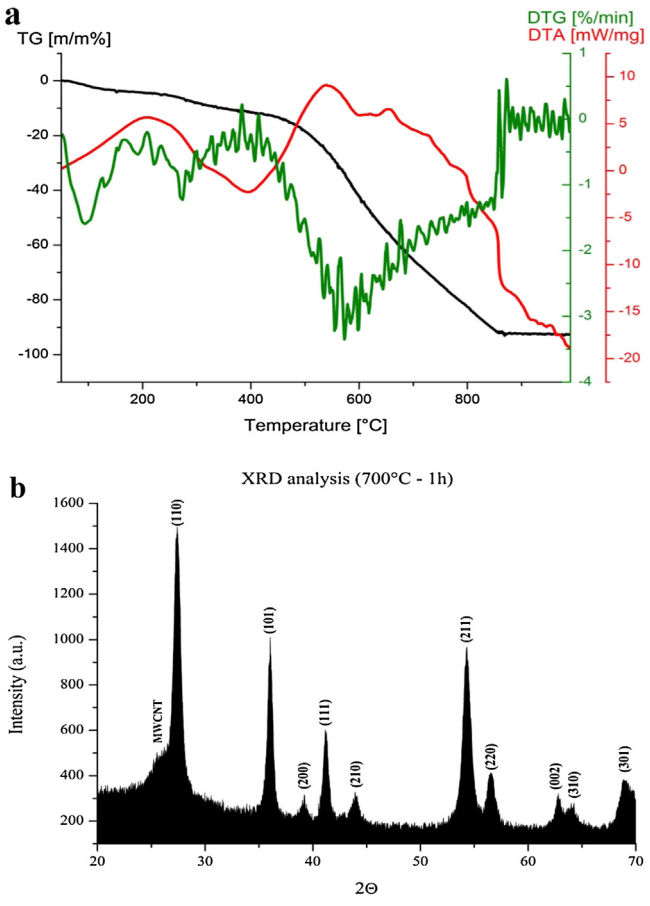

Fig. 2. a) Thermal analysis of TiO_2/MWCNT nanocomposite. b) XRD analysis of heat treated rutile/MWCNT nanocomposite film.

the diffraction peak at 2θ = 26.5° can be identified as the 002 reflection of MWCNTs. The other diffraction peaks in the range of 10° < 2θ < 70° correspond to the 110, 101, 200, 111, 210, 211, 220, 002, 310, 113, and 301 reflections of rutile [38], which indicate that nanoparticles on the surface of MWCNTs have rutile crystal structure. Furthermore, the average crystallite size can be estimated from Fig. 3b by Scherrer's formula:$D = (K\lambda) / (\beta\cos\Theta)$.

where D is the diameter (in nanometer) of the grain or the layer, K is the shape factor (0.89), λ is the X-ray wavelength of CuKα (0.154 nm), β is the experimental full-width half maximum of the respective diffraction peak(s), and Θ is the Bragg angle. The calculated mean particle size of TiO_2 was 9–10 nm.

3.2. SEM and EDS analysis

The fabrication of TiO_2/MWCNT composite films from ethanolic solution was successful using both of the precursor compounds, although different TiO_2 layer structures were observed during the SEM observations. SEM micrographs in Fig. 3 presents representative views of the composite films prepared with $TiOCl_2 \times 2HCl$ precursor and these images revealed the presence of titania coating formed on the surface of MWCNTs. After the analysis of the mentioned SEM images it was found that TiO_2 layers are partially broken with a size of 50–150 nm in the case of this precursor (marked by arrows in Figs. 3 a,d). The average diameter of the raw and covered MWCNTs and the prepared MWCNT films were calculated and based on these results it was possible to deduce the thickness of the TiO_2 coverage on the surface of the nanocomposite films. The average diameter of the raw CNTs was about 55–60 nm which was calculated with the analysis of SEM images by iTEM software. The diameter of MWCNTs covered in an atmosphere with 10% of RH was around 65–70 nm which can be seen in Fig. 3a. It means that TiO_2 layer was formed on the surface with a thickness of 10–15 nm. Increasing the RH from 10% to 50% the thickness of the TiO_2 layers on the surface of MWCNTs did not change significantly (Figs. 3a–e), although a slight growth of TiO_2 layers were observed.

Reaching 30% RH TiO_2 nanoparticles appeared not only on the surface of MWCNTs but also in the space between nanotubes (Fig. 3c). This undesired process is more intense at 40% RH (Fig. 3d). Because of the further increase of the RH (50%) bigger, individual and well distinguished TiO_2 aggregates were formed presumably due to the higher moisture content as it can be seen in Fig. 3e. In the case of 60% RH the whole surface was covered with coherent TiO_2 layer and we did not find individual or covered MWCNTs during investigations. This film is practically overcovered for further applications, thus not further analysed.

The observed phenomena between the cases of RH 30% and RH 50% were related to the increased relative humidity and the reactive $TiOCl_2 \times 2HCl$ precursor. As it is well-known titanium–halides can be easily hydrolysed. Based on this property it is strongly presumable that in case of higher RH values the hydrolysis of $TiOCl_2 \times 2HCl$ molecules is faster than the formation of chemical interaction between surface groups of MWCNTs and precursor compounds. Consequently, increasing the RH the TiO_2 surface layer could not be observed between the case of RH 40% and RH 50%. Early hydrolysis resulted in coalesced TiO_2 nanoparticles and undesired non uniform layer structures instead of homogeneously covered MWCNT films without separated inorganic particles in the case of RH 40%–50%, as it can be seen in Fig. 3d,e.

The comparable results of the SEM observations can be obtained (Fig. 4). These images indicate clearly that coatings originating from $TiBr_4$ provide more homogeneous coverages and the series of $TiBr_4$ precursor shows more uniform results. The thickness of the TiO_2 layers on the surface of nanocomposite films was also measured in each sample. After these measurements it was found that TiO_2 coverages formed on the surface of MWCNTs are thicker under any circumstances than in the samples prepared with use $TiOCl_2 \times 2HCl$ precursor. Presumably the solubility in ethanol and adsorption properties of $TiBr_4$ resulted in

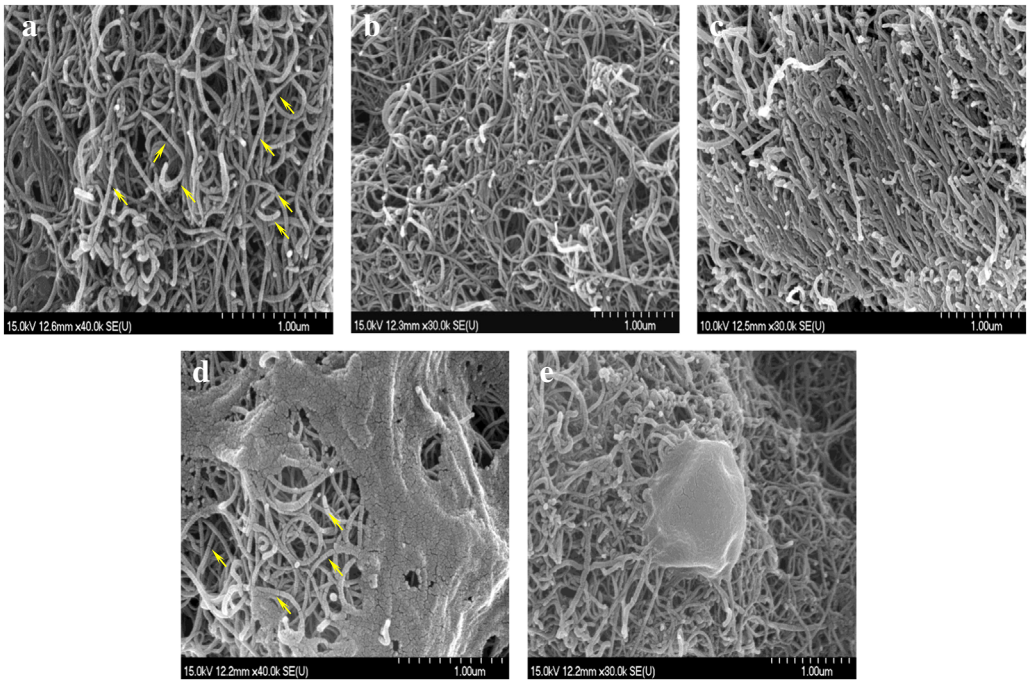

Fig. 3. SEM images of TiO_2/MWCNT films (precursor $TiOCl_2 \times 2H_2O$). a) RH 10%, b) RH 20%, c) RH 30%. d) RH 40%, e) RH 50%.

more homogeneous surface coverages and more integrated MWCNT films.

When the RH was 10% covered MWCNTs with a diameter of about 75–80 nm can be seen in Fig. 4a (the thickness of the TiO_2 layer was 20–25 nm). Using iTEM software it was determined that 10% increment of RH increases the thickness of the TiO_2 layers on the surface of MWCNTs with 5–10 nm (Fig. 4b). The thickness of TiO_2 layer on the surface of MWCNTs did not change with increasing the RH from 30% to 50%. In SEM images it can be clearly seen that TiO_2 nanoparticles began to fill the space between the MWCNTs when the relative humidity was 30% and 40% (Fig. 4c and d). In case of 50% RH it was observed that in addition to homogeneously covered MWCNTs the coherent TiO_2 layer was also formed on the surface of the nanocomposite film (Fig. 4e). It is important to highlight that between the cases of RH 30% and 50% larger separated agglomerates could not be observed during SEM investigations oppositely when the precursor was $TiOCl_2 \times 2HCl$. Furthermore, samples consist of fully covered MWCNTs as it can be visible in Fig. 4d and e. This observation and obtained structure could be especially advantageous during subsequent utilization. The sample prepared with a RH reaching 60% value consists of uncovered MWCNTs and bigger individual TiO_2 particles. The effect of relative humidity was the same which was observed in the case of $TiOCl_2 \times 2HCl$ and RH 60%.

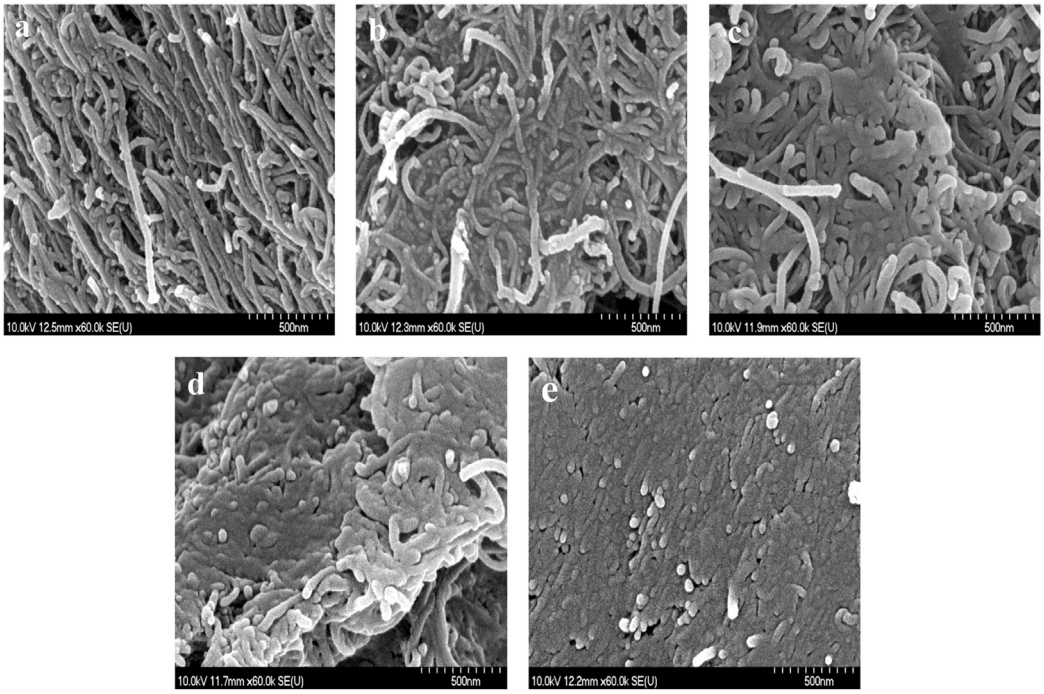

Fig. 4. SEM images of TiO_2/MWCNT films (precursor $TiBr_4$). a) RH 10%, b) RH 20%, c) RH 30%. d) RH 40%, e) RH 50%.

Our opinion is that due to the increased RH value the formation of separated titania particles becomes the preferred process inside the desiccators in case of both samples.

In order to characterize the quality of TiO_2 coating on the surface of MWCNTs, we performed energy dispersive X-ray analysis (EDS) by the SEM instrument for each samples. We present only three EDS spectra because of the similarity of the measured results (Figs. 5 a–c). The most significant signals originate from carbon (C), oxygen (O) and titanium (Ti), but another element, gold (Au) was also detected. The signal of gold is originated from the sputter coating process. EDS spectra shows (Fig. 5.) that raising the RH the quantity of TiO_2 increases which is in accordance with the thickness of the TiO_2 layers on SEM images.

3.3. Raman spectroscopy

The Raman spectra of the prepared samples confirm the presence of TiO_2 and MWCNT. Fig. 6 shows peaks and bands pointing at 235.7 cm^{-1}, 445.8 cm^{-1} and 608.8 cm^{-1} which are the characteristic peaks of the TiO_2 rutile phase [39,40]. Three other dominant bands deriving from MWCNTs appear at 1340.7 cm^{-1}, 1574.1 cm^{-1} and 2681 cm^{-1}, attributing to the D-, G- and G′-bands of MWCNTs, respectively. The purity of the MWCNT samples can be easily determined by the rations of these three peaks (Table 1). In case of MWCNTs the peak intensity ratios indicate good quality and highly graphitic nature. The change of the intensities in the spectrum of the sample TiO_2/MWCNT/50% RH can be assigned to the chemical interaction between TiO_2 and MWCNTs [41] by an inversion of the characteristic D/G, G′/G and D/G′ intensity ratios as it can be seen on Table 1. Probably due to the interaction between the MWCNTs and TiO_2 nanoparticles the bands slightly shifted [42].

4. Conclusion

In this study multi-walled carbon nanotube films were covered with titania under mild conditions. In order to fabricate accurately tailored inorganic layers, the effects of various titania precursors and a range of relative humidity was investigated. It can be concluded that samples prepared with $TiBr_4$ precursor provided more homogeneous surface coverages and more uniform MWCNT films in general. $TiBr_4$ as precursor formed completely homogeneous TiO_2 coating while in the case of

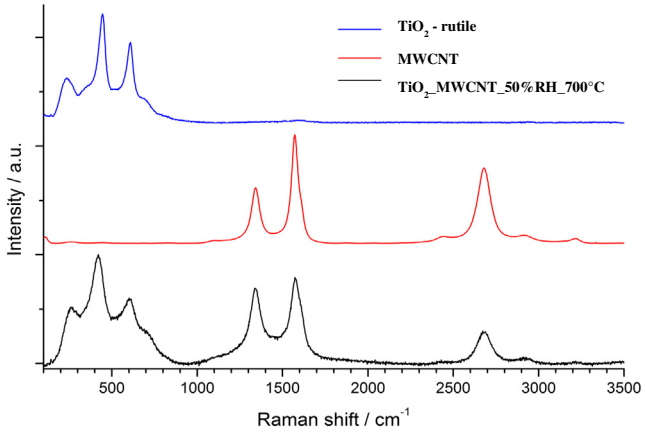

Fig. 6. Raman measurement which confirms that chemical bond formed between MWCNTs and rutile TiO_2 nanoparticles.

$TiOCl_2 \times 2HCl$ the resulting layers were slightly fragmented. Therefore changing the precursor we can easily control the type of TiO_2 coverage on the surface of MWCNT films. In addition, the formation of larger aggregates can be avoided successfully using $TiBr_4$ precursor in the range of RH 10% to 50%.

Due to the electron structure $TiBr_4$ has better sorption properties than $TiOCl_2 \times 2HCl$ and so it has consequently higher affinity to form more homogeneous and thicker TiO_2 layers on the surface of MWCNTs [17]. Furthermore, it is presumed that CNTs produced by CVD process contain significant amount of defect sites, which play an important role in the nucleation and firm binding of the TiO_2 layer. The chemical reaction between surface —OH or —COOH groups and titanium halide is strongly influenced by the RH, adsorption properties of reactants and the susceptibility to hydrolysis of the precursor compounds.

TiO_2 layer produced with $TiBr_4$ is approximately 10–15 nm thicker than the layer originated from $TiOCl_2 \times 2HCl$ precursor. By varying the RH from 10% to 60% and applying a sealed system we proved that the relative humidity is an important parameter during the preparation. The thickness and the quality of the resulting TiO_2 layers are more controllable by using $TiBr_4$ precursor. Reaching 50% of RH formation of segregated TiO_2 particles becomes the preferred process in case of both

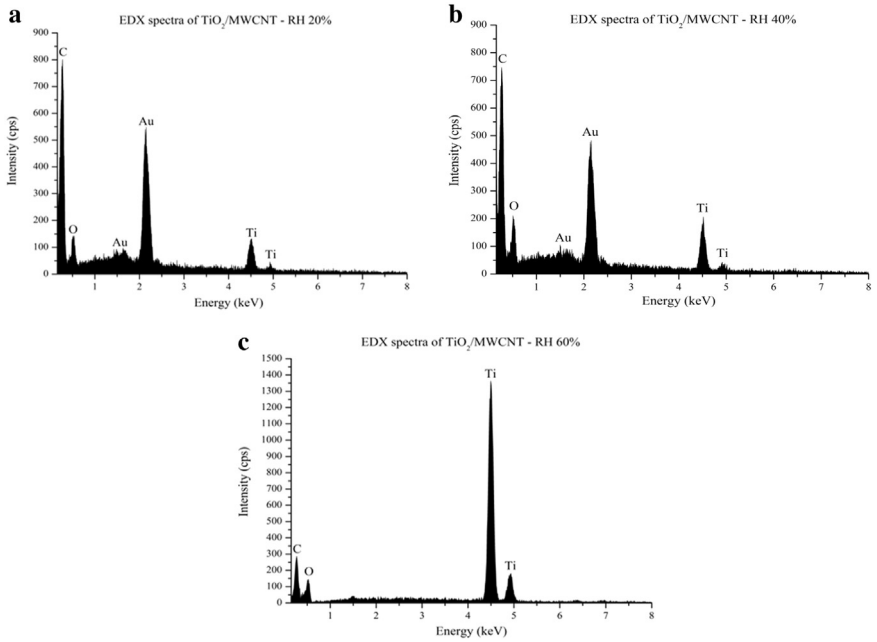

Fig. 5. a) EDS spectra of TiO_2/MWCNT film obtained at RH 20%. b) EDS spectra of TiO_2/MWCNT film, —″ —RH 40%. c) EDS spectra of TiO_2/MWCNT film, —″. —RH 60%.

Table 1
Summary of the ratios of the D, G and G′ peaks.

	Pristine MWCNT	TiO_2/MWCNT 50% RH
I_D/I_G	0.51	0.88
$I_{G'}/I_G$	0.69	0.38
$I_D/I_{G'}$	0.74	2.31

precursor due to the increased water content and the reactivity of titanium halides.

Raman spectroscopy measurements confirm that the intensity of the D-band of TiO_2 coated MWCNTs is higher than in the spectrum of original CNTs, probably due to the influence of the interaction between TiO_2 nanoparticles and carbon nanotubes. XRD measurements proved that TiO_2 nanoparticles were in rutile phase and the calculated mean particle size of TiO_2 nanoparticles was 9–10 nm.

Our conclusion is that $TiBr_4$ can be considered as an excellent precursor compound for covering MWCNTs and the surface layer structure of the membranes can be influenced properly applying different RH values and $TiBr_4$ as precursor. TiO_2/MWCNT nanocomposite membranes could be used as promising materials for environmental cleaning since MWCNTs could efficiently adsorb pollutants in water and also increase the photocatalytic activity of TiO_2 by acting as electron traps [43], thus stabilizing the charge carriers and suppressing the rate of electron–hole recombination.

Acknowledgments

The work was supported by the Swiss Contribution SH/7/2/20. Zoltán Németh is funded by Sciex project no. 14.119. Balázs Réti is thankful for the financial support from the Social Renewal Operational Programme of Hungary (TÁMOP-4.2.2.A-11/1/KONV-2012-0047).

References

[1] R. Saito, M.S. Dresselhaus, G. Dresselhaus, Physical Properties of Carbon Nanotubes, Imperial College Press, UK, 1998.
[2] P.M. Ajayan, O.Z. Zhou, Applications of carbon nanotubes. Carbon nanotubes, topics, Appl. Phys. 80 (2001) 391–425.
[3] M.F.L. Volder, S.H. Tawfick, R.H. Baughman, A.J. Hart, Carbon nanotubes: present and future commercial applications, Science 339 (2013) 535–539.
[4] C.W. Tan, K.H. Tan, Y.T. Ong, A.R. Mohamed, S.H. Zein, S.H. Tan, Energy and environmental applications of carbon nanotubes, Environ. Chem. Lett. 10 (2012) 265–273.
[5] M.S. Rahaman, C.D. Vecitis, M. Elimelech, Electrochemical carbon-nanotube filter performance toward virus removal and inactivation in the presence of natural organic matter, Environ. Sci. Technol. 46 (3) (2012) 1556–1564.
[6] A.S. Brady-Este'vez, M.H. Schnoor, C.D. Vecitis, N.B. Saleh, M. Elimelech, Multiwalled carbon nanotube filter: improving viral removal at low pressure, Langmuir 26 (2010) 14975–14982.
[7] A.S. Brady-Este'vez, M.H. Schnoor, S. Kang, M. Elimelech, SWNT–MWNT hybrid filter attains high viral removal and bacterial inactivation, Langmuir 26 (2011) 19153–19158.
[8] K.T. Park, J. Hwang, Filtration and inactivation of aerosolized bacteriophage MS2 by a CNT air filter fabricated using electro-aerodynamic deposition, Carbon 75 (2014) 401–410.
[9] G. Gao, Q. Zhang, C.D. Vecitis, CNT-PVDF composite flow-through electrode for single-pass sequential reduction-oxidation, J. Mater. Chem. A 2 (2014) 6185–6190.
[10] K. Hernadi, E. Ljubovic, J.W. Seo, L. Forro, Synthesis of MWNT-based composite materials with inorganic coating, Acta Mater. 51 (2003) 1447–1452.
[11] M.S. Mauter, M. Elimelech, Environmental applications of carbon-based nanomaterials, Environ. Sci. Technol. 42 (16) (2008) 5843–5859.
[12] B. Chen, S. Li, H. Imai, L. Jia, J. Umeda, M. Takahashi, K. Kondoh, An approach for homogeneous carbon nanotube dispersion in Al matrix composites, Mater. Des. 72 (2015) 1–8.
[13] R. Rahmanian, A.R. Suraya, M.A. Shazed, R. Zahari, E.S. Zainudin, Mechanical characterization of epoxy composite with multiscale reinforcements: carbon nanotubes and short carbon fibers, Mater. Des. 60 (2014) 34–40.
[14] B. O'Regan, M. Grätzel, A low-cost, high-efficiency solar cell based on dye-sensitized, Nature 353 (1991) 737.
[15] X. Qu, J. Brame, Q. Li, P.J.J. Alvarez, Nanotechnology for a safe and sustainable water supply: enabling integrated water treatment and reuse, Acc. Chem. Res. 46 (3) (2013) 834–843.
[16] B. Reti, K. Mogyorosi, A. Dombi, K. Hernadi, Substrate dependent photocatalytic performance of TiO_2/MWCNT photocatalysts, Appl. Catal. A 469 (2014) 153–158.
[17] B. Gao, G.Z. Chen, G.L. Puma, Carbon nanotubes/titanium dioxide (CNTs/TiO_2) nanocomposites prepared by conventional and novel surfactant wrapping sol–gel methods exhibiting enhanced photocatalytic activity, Appl. Catal. B 89 (2009) 503–509.
[18] M.Q. Yang, N. Zhang, Y.J. Xu, Synthesis of fullerene-, carbon nanotube-, and graphene-TiO_2 nanocomposite photocatalysts for selective oxidation: A comparatice study, Appl. Mater. Interfaces 5 (3) (2013) 1156–1164.
[19] S. Aryal, C.K. Kim, K.W. Kim, M.S. Khil, H.Y. Kim, Multi-walled carbon nanotubes/TiO_2 composite nanofiber by electrospinning, Mater. Sci. Eng. C 28 (2008) 75–79.
[20] L.C. Jiang, W.D. Zhang, A highly sensitive nonenzymatic glucose sensor based on CuO nanoparticles-modified carbon nanotube electrode, Electroanal 21 (2009) 988–993.
[21] K. Byrappa, A.S. Dayananda, C.P. Sajan, B. Basavalingu, M.B. Shayan, K. Soga, M. Yoshimura, Hydrothermal preparation of ZnO:CNT and TiO_2:CNT composites and their photocatalytic applications, J. Mater. Sci. 43 (2008) 2348–2355.
[22] S.D. Perera, R.G. Mariano, K. Vu, N. Nour, O. Seitz, Y. Chabal, K.J. Balkus, Hydrothermal synthesis of graphene-TiO_2 nanotube composites with enhanced photocatalytic activity, ACS Catal. 2 (6) (2012) 949–956.
[23] L. Chen, B.L. Zhang, M.Z. Qu, Z.L. Yu, Preparation and characterization of CNTs–TiO_2 composites, Powder Technol. 154 (2005) 70–72.
[24] Y. Yu, J.C. Yu, C.Y. Chan, Y.K. Che, J.C. Zhag, L. Ding, W.K. Ge, P.K. Wong, Enhancement of adsorption and photocatalytic activity of TiO_2 by using carbon nanotubes for the treatment of azo dye, Appl. Catal. B 61 (2005) 1–11.
[25] S. Dörfler, M. Hagen, H. Althues, J. Tübke, S. Kaskel, M.J. Hoffmann, High capacity vertical aligned carbon nanotube/sulfur composite cathodes for lithium–sulfur batteries, Chem. Commun. 48 (2012) 4097–4099.
[26] K.E. Tettey, M.Q. Yee, D. Lee, Photocatalytic and conductive MWCNT/TiO_2 nanocomposite thin films, Appl. Mater. Interfaces 2 (9) (2010) 2646–2652.
[27] H. Yu, X. Quan, S. Chen, H. Zhao, Y. Zhang, TiO_2–carbon nanotube heterojunction arrays with a controllable thickness of TiO_2 layer and their first application in photocatalysis, J. Photochem. Photobiol. A Chem. 200 (2008) 301–306.
[28] W. Wang, P. Serp, P. Kalck, J.L. Faria, Photocatalytic degradation of phenol on MWNT and titania composite catalysts prepared by a modified sol–gel method, Appl. Catal. B Environ. 56 (2005) 305–312.
[29] D. Eder, A.H. Windle, Morphology control of CNT–TiO_2 hybrid materials and rutile nanotubes, J. Mater. Chem. 18 (2008) 2036–2043.
[30] G. An, W. Ma, Z. Sun, Z. Liu, B. Han, S. Miao, Z. Miao, K. Ding, Preparation of titania/carbon nanotube composites using supercritical ethanol and their photocatalytic activity for phenol degradation under visible light irradiation, Carbon 45 (2007) 1795–1801.
[31] W. Zhang, Y. Chen, S. Yu, S. Chen, Y. Yin, Preparation and antibacterial behavior of Fe^{3+}-doped nanostructured TiO_2 thin films, Thin Solid Films 516 (2008) 4690–4694.
[32] B. Korbely, Z. Nemeth, B. Reti, J.W. Seo, A. Magrez, L. Forro, K. Hernadi, Fabrication of homogeneous titania/MWNT composite materials, Mater. Res. Bull. 46 (2011) 1991–1996.
[33] Z. Nemeth, C. Dieker, A. Kukovecz, D. Alexander, L. Forro, J.W. Seo, K. Hernadi, Preparation of homogeneous titania coating on the surface of MWNT, Comput. Sci. Technol. 71 (2011) 87–94.
[34] E. Couteau, K. Hernadi, J.W. Seo, L. Thien-Nga, Miko Cs, R. Gaál, L. Forró, CVD synthesis of high-purity multiwalled carbon nanotubes using $CaCO_3$ catalyst support for large-scale production, Chem. Phys. Lett. 378 (2003) 9–17.
[35] A. Magrez, J.W. Seo, Miko Cs, K. Hernadi, L. Forro, Growth of carbon nanotubes with alkaline earth carbonate as support, J. Phys. Chem. B 109 (2005) 10087–10091.
[36] M.S. Dresselhaus, G. Dresselhaus, R. Saito, A. Jorio, Raman spectroscopy of carbon nanotubes, Phys. Rep. 409 (2) (2005) 47–99.
[37] M.E. Solomon, Control of humidity with potassium hydroxide, sulphuric acid, or other solutions, Bull. Entomol. Res. 42 (1951) 543–554.
[38] J. Yan, G. Wu, N. Guan, L. Li, Z. Li, X. Cao, Understanding the effect of surface/bulk defects on the photocatalytic activity of TiO_2: anatase versus rutile, Phys. Chem. Chem. Phys. 15 (2013) 10978–10988.
[39] C.A. Melendres, A. Narayanasamy, V.A. Maroni, R.W. Siegel, Raman spectroscopy of nanophase TiO_2, J. Mater. Res. 4 (1989) 1246–1250.
[40] E.H. Poniatowski, R.R. Talavera, M.C. Heredia, O.C. Coro, Crystallization of nanosized titania particles prepared by the sol–gel process, J. Mater. Res. 9 (1994) 2102–2108.
[41] F. Inoue, R.A. Ando, P. Corio, Raman evidence of the interaction between multiwalled carbon nanotubes and nanostructured TiO_2, J. Raman Spectrosc. 42 (2011) 1379–1383.
[42] Y.D. Yang, L.T. Qu, L.M. Dai, T.S. Kang, M. Durstock, Electrophoresis coating of titanium dioxide on aligned carbon nanotubes for controlled syntheses of photoelectronic nanomaterials, Adv. Mater. 19 (2007) 1239–1243.
[43] M. Hamadanian, M. Shamshiri, V. Jabbari, Novel high potential visible-light-active photocatalyst of CNT/Mo, S-codoped TiO_2 hetero-nanostructure, Appl. Surf. Sci. 317 (2014) 302–311.